Vol. 2 No. 1 page 67-73
DOI: 10.14456/randk.2016.9

RESEARCH & KNOWLEDGE

Research Article

Pulse wave propagation and velocity in aneurysmal aorta using FSI model

Tipapon Khamdaeng[1,*], Numpon Panyoyai[1], Thanasit Wongsiriamnuay[1] and Pradit Terdtoon[2]

[1] Department of Agricultural Engineering, Maejo University, Chiang Mai, Thailand
[2] Department of Mechanical Engineering, Chiang Mai University, Chiang Mai, Thailand

(Received 19 November 2015; accepted 25 December 2015)

Abstract - The pulse wave velocity (PWV) has been shown to be associated with the properties of blood vessels and a cardiovascular risk factor, such as an aneurysm. The global PWV estimation is applied in conventional clinical diagnosis. However, the geometry of the blood vessel changes along the wave traveling path and the global PWV estimation may not always detect regional wall changes resulting from cardiovascular diseases. In this study, a fluid structure interaction (FSI) analysis was applied on straight-shaped aortas with and without an aneurysm with the aim of determining the effects of the aneurysm size and the ratio of the aneurysm to wall modulus on the pulse wave propagation and velocity. The characterization for each stage of the aneurysmal aorta was simulated by progressively increasing aortic stiffness and aneurysm size. The pulse wave propagations and velocities were estimated from a two-dimensional spatial-temporal plot of the normalized wall displacement based on elastic deformation. The supra- and infra-aneurysm PWVs of aneurysmal aortic walls were found to be up to 58±14% and 13±10%, respectively, which were different from the PWV of a normal aortic wall. The combined quantitative and qualitative parameters, i.e., PWV, magnitude of wall displacement on the wave, width of the standing wave and wave propagations, were used to distinguish the characterization of the normal and aneurysmal aortic walls and shown to be relevant regional markers that can be utilized in clinical diagnosis.

Keywords: Aneurysm, heterogeneous aortic wall, pressure wave, stiffness

1. Introduction

Arterial stiffness is used worldwide as an indicator associated with the onset and progression of cardiovascular diseases, such as aortic aneurysms, thrombosis, stenosis, atherosclerosis and coronary events, etc. Several *in vivo* noninvasive methods have been proposed to assess the arterial stiffness, such as pulse wave imaging (PWI) (Shahmirzadi *et al*., 2013; Vappou *et al*., 2010), pressure-diameter (Nichols and O'Rourke, 2005) or stress-strain relationship (Danpinid *et al*., 2010; Khamdaeng *et al*., 2012), based ultrasound. The conventional *in vivo* noninvasive method is the global measurement of the pulse wave velocity (PWV). The pulse wave profiles of arterial wall pressure can be continuously measured by using applanation tonometry at two distant locations, e.g., carotid and femoral arteries. To obtain the pulse wave velocity, the distance between the two different locations is divided by the traveling time delay. Using a modified Moens-Korteweg equation, the pulse wave velocity can be related to the arterial stiffness (Nichols and O'Rourke, 2005). Although applanation tonometry has been used in routine clinical studies, it is limited by the uncertainty of the path traveled by the pulse wave velocity, i.e., the arterial wall geometry changes between the two measurement points, thus, the diseases may not always be located along the travel line of the pulse wave (Luo *et al*., 2009). There are a few regional noninvasive measurements using ultrasound and MRI-based methods (Markl *et al*., 2010; Fujikura *et al*., 2007; Li *et al*., 2011) to locally detect the changes in stiffness. The pulse wave velocity is not only quantitatively determined but also the pulse wave propagation can be qualitatively visualized. The abnormalities, changes in mechanical properties, of the regional arterial wall can be identified and localized. The changes in the propagation speed and patterns of the pulse wave velocity were found to be clear markers to detect the regional abnormalities (Baquet, 2003; Williams, 2007). Methods involving assessments of regional aortic stiffness have been proposed and developed to be applied in clinical detection. The regional pulse wave propagation and velocity of normal and aneurysmal aortas were investigated in mice and humans using pulse wave imaging validated by simulation and phantom findings (Vappou *et al*., 2011; Luo *et al*., 2008; Shahmirzadi *et al*., 2012). The fluid-structure interaction (FSI) finite-element simulation was shown to be a reliable tool to obtain the pulse wave propagation on aorta with homogeneous and non-homogeneous walls and

*Author for correspondence: tipapon@mju.ac.th

to serve as a guide for pulse wave imaging *in vivo* (Khamdaeng *et al*., 2015; Shahmirzadi and Konofagou, 2012; Shahmirzadi and Konofagou, 2014). Due to the complexity of blood flow in arteries, the model of the luminal pressure variations with altered hemodynamics is utilized to realistically simulate the fluid-solid arterial responses. A reliable three-dimensional aortic model with normal and pathological aortas is therefore required to visualize and measure the regional pulse wave propagation and velocity. Therefore, the objective of this study was to investigate the pulse wave propagation and velocity in straight-shaped aortas with and without aneurysm using a coupled dynamic FSI model.

2. Fluid structure interaction (FSI) model

The aortic wall was assumed to be one axisymmetric layer that exhibited nonlinear elastic behavior. The aortic geometry and boundary conditions under consideration are shown in Figure 1. The luminal diameter, d_i, was equal to 16 mm along with the longitudinal length, L, of 300 mm. The wall thickness, t, was equal to 2.2 mm (Fig. 1a). The aortic wall was modeled with wall density ϱ_s = 1050 kg/m^3, Poisson's ratio υ = 0.48 and Young's modulus E_{normal} = 2.56 MPa, representing a normal wall (Humphrey, 2002). The non-homogeneous models were assumed to have the aneurysm size of axial lengths L_a = 25, 37.5 and 50 mm (Fig. 1b, 1c and 1d), which was located at 50 mm from the tube inlet. Young's moduli of E_{stiff} = 2.56, 5.12, 7.68 and 10.24 MPa (Shahmirzadi and Konofagou, 2012) were used to represent the aneurysmal stiffness. The extravascular pressure was assumed to be null. The fluid was modeled as Newtonian with material properties of fluid density ϱ_f equal to 1000 kg/m^3, reference speed of sound, c_o, was equal to 1483 m/s and fluid viscosity η = 0.0001 Ns/m^2 (Kanyanta, *et al*., 2009).

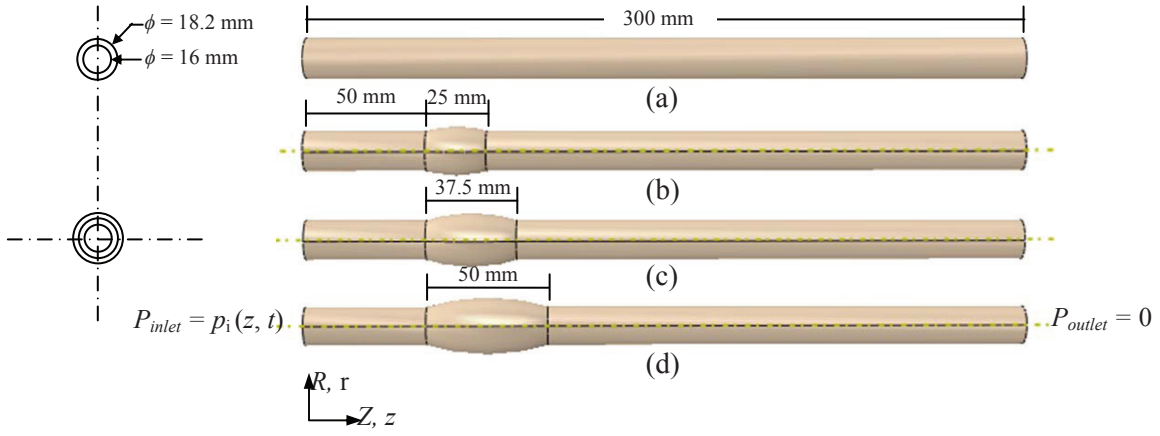

Figure 1. Schematic illustration of aortic models and specified boundary conditions with (a) homogeneous model. Non-homogeneous model with aneurysm size of axial length, L_a, of (b) 25, (c) 37.5 and (d) 50 mm.

Both inlet and outlet ends were fully constrained in three dimensions. A time dependent fully developed fluid pulse pressure was applied on the tube inlet. The fluid structure interface was defined as frictionless. The hexagonal 3D elements were meshed with a seeding size of 1 mm. 34800 and 48900 elements were respectively generated on the aortic wall and fluid parts for the normal homogeneous model. The number of elements was changed between 33900 to 34226 and 49063 to 49500 on the aortic wall and fluid parts, respectively, across the non-homogeneous models. The initial time increment was 6.743×10^{-7} s. 3D coupled simulations were performed. Nodes along the axial length of the tube were selected to determine the displacement in the radial direction at each time increment (Fig. 2). The wave propagation was mapped on a 2D plane, with time and axial location as the x and y axes, respectively. The wave peak at each time increment could be visualized and tracked. Therefore, the pulse wave velocity could be determined as the slope of the axial locations of the wave peak and time relation.

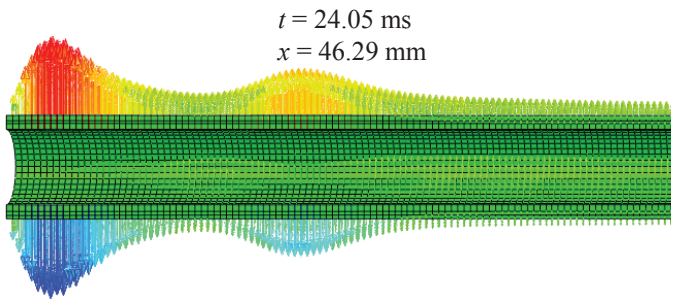

Figure 2. Example of pulse pressure wave induced wall displacement in radial direction at any time increment along the tube. The arrows denote the magnitude of the wall displacement.

3. Results and Discussion

3.1 Pulse wave propagation and velocity

The pulse wave propagation and velocity of the aortic wall with and without aneurysm were investigated in this study. The coupled fluid structure interaction model was used to describe the compliant aortic wall phenomenon induced by pulsatile blood pressure.

Figure 3(a) illustrates the 2D spatial-temporal plot of the normalized wall displacement of the homogeneous aortic wall with E_{normal} equal to 2.56 MPa. The relationship between the axial location and time was fitted using a linear regression model to yield the pulse wave velocity. The forward pulse wave velocity was found to be equal to 2.380 m/s.

The non-homogeneous walls with aneurysm size L_a = 25, 37.5 and 50 mm of aneurysmal stiffness E_{stiff} = 10.24 MPa and walls with aneurysmal stiffness E_{stiff} = 2.56, 5.12, 7.68 and 10.24 MPa of aneurysm size L_a = 25 mm are shown in Figure 3(b)-3(d) and Figure 3(e)-3(h), respectively. The reflected, supra-, infra- and within-aneurysm waves were observed. The supra-aneurysm wave traveled toward the aneurysm and separated into three portions. The first portion was reflected at the inlet aneurysm site and traveled backward. The other portions, i.e., within- and infra-aneurysm waves, were maintained forward traveling. The pulse wave velocities of the reflected, supra-, infra-, and within-aneurysm waves obtained from the linear fits are shown in Table 1.

The fluid structure interaction framework was previously used to investigate the pulse wave propagation and velocity on the aortic walls with and without inclusions. The present study reports the effects of the aneurysm size and the ratio of aneurysm to wall modulus on the pulse wave propagation and velocity to serve as a guide for pulse wave imaging *in vivo*. The forward wave was only observed on the homogeneous model, unlike the case of the non-homogeneous models. The hard-stiff aneurysms caused the reflected wave, but they did not cause remarkable changes in the pulse wave velocity, which was the same as the within-aneurysm wave. The changes in the ratio of the aneurysm to wall modulus and the aneurysm size caused the changes in the pulse wave velocity of the supra- and infra-aneurysm waves, respectively, which are better shown as evident markers.

3.2 Effect of aneurysm size

To investigate the effect of the aneurysm size on the pulse wave propagation and velocity, the 2D spatial-temporal plots of the normalized wall displacement of the non-homogeneous aortic wall with aneurysm size L_a = 25, 37.5, and 50 mm of aneurysmal stiffness E_{stiff} = 10.24 MPa (Figure 3(b)-3(d)) were demonstrated. Figure 4(a) illustrates the effect of the aneurysm size on the pulse wave propagation and velocity. The pulse wave velocity of the infra-aneurysm and reflected waves decreased when the aneurysm size increased. The supra- and within-aneurysm waves were found to slightly increase in pulse wave velocity with the aneurysm size. The standing wave was found to occur at the inlet aneurysm site, with its width increasing with an increase in the aneurysm size. A small aneurysm size with hard stiffness showed a nonlinearity for the infra-aneurysm pulse wave velocity, and there was a better fit with two linear correlations. The change in pulse wave velocity of the infra-aneurysm wave was found up to 70%, which indicated the highest sensitivity to change in the aneurysm size.

3.3 Effect of ratio of aneurysm to wall modulus

The 2D spatial-temporal plots of the normalized wall displacement of the non-homogeneous aortic wall with aneurysmal stiffness E_{stiff} = 2.56, 5.12, 7.68, and 10.24 MPa of aneurysm size L_a = 25 mm are shown in Figure 3(e)-3(h). Figure 4(b) illustrates the effect of the ratio of the aneurysm to the wall modulus on the pulse wave propagation and velocity. The change in the ratio of the aneurysm to wall modulus was found to be the least likely to be detected by the pulse wave velocity of the reflected, infra-, and within-aneurysm waves. However, the nonlinearity of the infra-aneurysm pulse wave velocity was found to increase with an increase in the ratio of the aneurysm to wall modulus, which can be better fitted with two linear correlations. The magnitude of wall displacement on the reflected wave also increased with the ratio of aneurysm to wall modulus. The pulse wave velocity of the supra-aneurysm wave decreased up to 100% when the ratio of the aneurysm to wall modulus increased and its change indicated the highest sensitivity to change in the ratio of the aneurysm to the wall modulus.

Table 1. Pulse wave propagation and velocity (PWV) of seven aortic models with homogeneous and non-homogeneous models.

Aortic model	Young's modulus (MPa)	Aneurysm size (mm)	Wave type	PWV (m/s)
Homogeneous	Aortic wall: 2.56	-	Forward	2.380
Non-homogeneous with aneurysm	Aortic wall: 2.56 Aneurysm: 2.56	25	Supra-aneurysm: Forward Within-aneurysm: Forward Infra-aneurysm: Forward	 1.631 0.239 2.532
	Aortic wall: 2.56 Aneurysm: 5.12	25	Supra -aneurysm: Forward Reflected Within-aneurysm: Forward Infra-aneurysm: Forward	 1.250 1.675 0.241 2.494
	Aortic wall: 2.56 Aneurysm: 7.68	25	Supra -aneurysm: Forward Reflected Within-aneurysm: Forward Infra-aneurysm: Forward	 1.046 1.640 0.353 2.535
	Aortic wall: 2.56 Aneurysm: 10.24	25	Supra -aneurysm: Forward Reflected Within-aneurysm: Forward Infra-aneurysm: Forward	 0.602 1.625 0.382 2.595
	Aortic wall: 2.56 Aneurysm: 10.24	37.5	Supra -aneurysm: Forward Reflected Within-aneurysm: Forward Infra-aneurysm: Forward	 0.922 1.135 0.552 1.989
	Aortic wall: 2.56 Aneurysm: 10.24	50	Supra -aneurysm: Forward Reflected Within-aneurysm: Forward Infra-aneurysm: Forward	 0.945 1.176 0.900 1.524

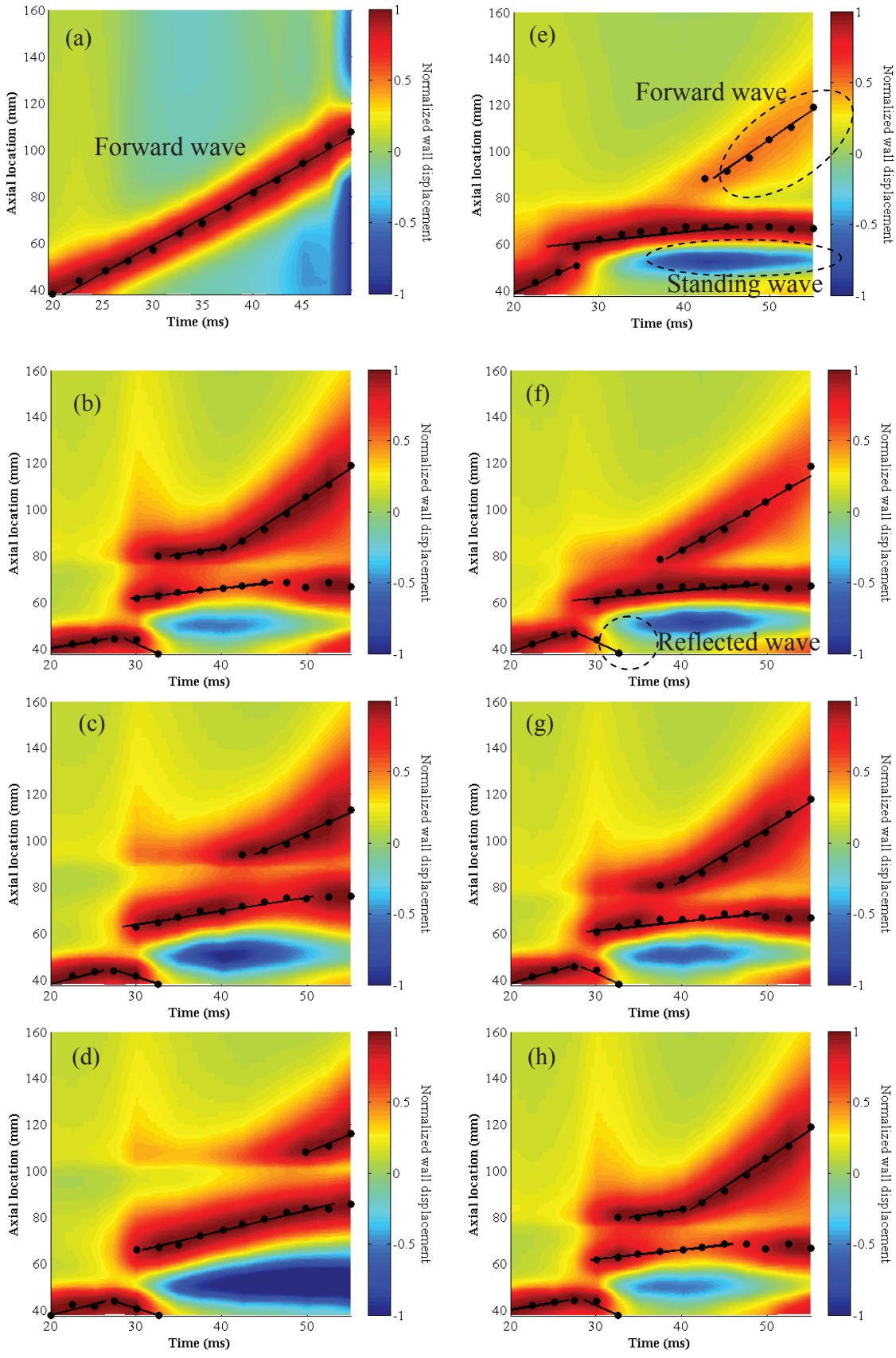

Figure 3. 2D spatial-temporal plot of normalized wall displacement (wave peaks are shown) of (a) homogeneous wall (E_{normal} = 2.56 MPa); walls with L_a equal to (b) 25, (c) 37.5, and (d) 50 mm of E_{stiff}= 10.24 MPa; and walls with E_{stiff} equal to (e) 2.56, (f) 5.12, (g) 7.68, and (h) 10.24 MPa of L_a=25 mm. The fitting yields the pulse wave velocity.

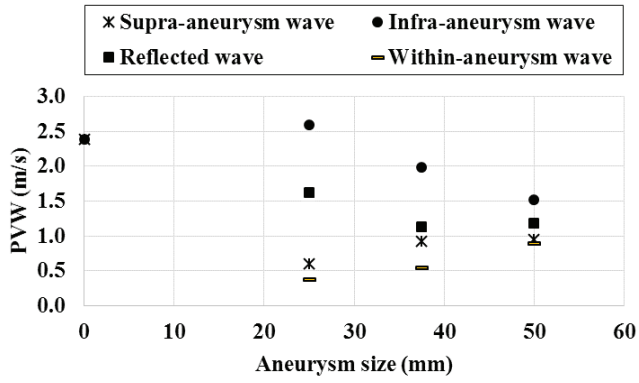

(a)

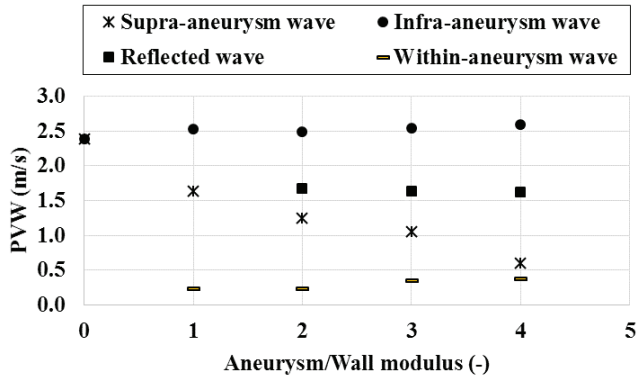

(b)

Figure 4. Effects of (a) aneurysm size and (b) ratio of aneurysm to wall modulus on pulse wave velocity.

4. Conclusion

Normal homogeneous and aneurysmal non-homogeneous aortic models were successfully established to estimate the pulse wave velocity propagation and velocity using a fluid structure interaction (FSI) simulation. The 2D spatial-temporal plot of the normalized wall displacement provided clear information on the regional pulse wave propagation. The effects of the aneurysm size and the ratio of the aneurysm to the wall modulus on the pulse wave propagation and velocity were examined. The changes of the aneurysm size and the ratio of aneurysm to wall modulus were qualitatively identified by the reflected wave and standing wave propagations. The quantitative results, such as, pulse wave velocity, magnitude of wall displacement on the wave, and width of the standing wave, were determined. The interpretations from both qualitative and quantitative results were found to be able to differentiate between the homogeneous and non-homogeneous models. The distinction between the aneurysm size and the ratio of the aneurysm to the wall modulus was characterized.

Acknowledgements

This study was supported in part by the Thailand Research Fund (TRF) and the Faculty of Engineering and Agro-Industry, Maejo University, Chiang Mai, Thailand.

References

Baquet, J. P., Kingwell, B. A., Dart, A. L., Shaw, J., Ferrier, K. E. and Jennings, G. L. 2003. Analysis of the regional pulse wave velocity by Doppler: methodology and reproducibility. Journal of Human Hypertension 17, 407-412.

Danpinid, A., Luo, J.,Vappou, J., Terdtoon, P. and Konofagou, E. E. 2010. In vivo characterization of the aortic wall stress-strain relationship. Ultrasonics 50, 654-665.

Fujikura, K., Luo, J., Gamarnik, V., Pernot, M., Fukumoto, R., Tilson III, M. and Konofagou, E. E. 2007. A novel noninvasive technique for pulse-wave imaging and characterization of clinically-significant vascular mechanical properties in vivo. Ultrasound Imaging 29(3), 137- 154.

Humphrey, J. 2002. Cardiovascular solid mechanics: cells, tissues, and organs, Springer-Verlag, New York.

Kanyanta, V., Ivankovic, A. and Karac, A. 2009. Validation of a fluid-structure interaction numerical model for predicting flow transients in arteries. Journal of Biomechanics, 42(11), 1705-1712.

Khamdaeng, T., Luo, J., Vappou, J., Terdtoon, P. and Konofagou, E. E. 2012. Arterial stiffness identification of the human carotid artery using the stress-strain relationship in vivo. Ultrasonics 52, 402-411.

Khamdaeng, T., Panyoyai, N.,Wongsiriamnuay, T., and

Terdtoon, P. 2015. Pulse wave propagation and velocity in arch-shaped aorta. Rajamangala University of Technology Isan Journal 8, 51-62.

Li, R. X., Luo, J., Khamdaeng, T. and Konofagou, E. E. 2011. Pulse wave imaging (PWI) and arterial stiffness measurement of the human carotid artery: an in vivo feasibility study. In: Proceedings of the IEEE International Ultrasonics Symposium 2011 (IUS 2011), Caribe Royale, Orlando, Florida, USA, pp. 1778-1781.

Luo, J., Fujikura, K., Tyrie, L. S., Tilson, M. D. and Konofagou, E. E. 2009. Pulse wave imaging of normal and aneurysmal abdominal aortas in vivo. IEEE Transactions on Medical Imaging 28, 477-486.

Luo, J., Lee, W. N., Wang, S. and Konofagou, E. E. 2008. Pulse wave imaging of human abdominal aortas in vivo. In: Proceedings of the IEEE International Ultrasonics Symposium 2008 (IUS 2008), Beijing, China, pp. 859-862.

Markl, M., Wallis, W., Brendecke, S., Simon, J., Frydrychowicz, A. and Harloff, A. 2010. Estimation of global aortic pulse wave velocity by flow-sensitive 4D MRI. Magnetic Resonance in Medicine 63(6), 1575-1582.

Nichols, W.W. and O'Rourke, M.F. 2005. Mc Donald's blood flow in arteries: theoretical, experimental, and clinical principles, 5th ed. A Hodder Arnold Publication, London, 67-76.

Shahmirzadi, D. and Konofagou, E. E. 2014. Quantification of arterial wall inhomogeneity size, distribution, and modulus contrast using FSI numerical pulse wave propagation. Artery Research 8, 57-65.

Shahmirzadi, D. and Konofagou, E. E. 2012. Detection of aortic wall inclusions using regional pulse wave propagation and velocity in silico. Artery Research 6, 114-123.

Shahmirzadi, D., Li, R. X. and Konofagou, E. E., 2012. Pulse-wave propagation in straight-geometry vessels for stiffness estimation: theory, simulations, phantoms and in vitro findings. Journal of Biomedical Engineering 134(11), 114502.

Shahmirzadi, D., Narayanan, P., Li, R. X., Qaqish, W. W. and Konofagou, E. E. 2013. Mapping the longitudinal wall stiffness heterogeneities within intact canine aortas using Pulse Wave Imaging (PWI) ex vivo. Journal of Biomechanics 46, 1866-1874.

Vappou, J., Luo, J., Okajima, K., Tullio, M. D. and Konofagou, E. E. 2011. Aortic pulse wave velocity measured by pulse wave imaging (PWI): a comparison with applanation tonometry. Artery Research 5, 65-71.

Vappou, J., Luo, J. and Konofagou, E. E. 2010. Pulse wave imaging for noninvasive and quantitative measurement of arterial stiffness in vivo. American Journal of Hypertension 23, 393-398.

Williams, R., Needles, A., Cherin, E., Zhou, Y. Q., Henkelman, R. M., Adamson, S. E. and Foster, F. S. 2007. Noninvasive ultrasonic measurement of regional and local pulse-wave velocity in mice. Ultrasound in Medicine & Biology 33(9), 1368-1375.